Targeted deletion of endothelial lipase increases HDL particles with anti-inflammatory properties both in vitro and in vivo

Tetsuya Hara,* Tatsuro Ishida,[1,*] Yoko Kojima,* Hanayo Tanaka,* Tomoyuki Yasuda,* Masakazu Shinohara,*[,†] Ryuji Toh,* and Ken-ichi Hirata*

Division of Cardiovascular Medicine,* and the Integrated Center for Mass Spectrometry,[†] Kobe University Graduate School of Medicine, Kobe, Japan

Abstract **Previous studies have shown that targeted deletion of endothelial lipase (EL) markedly increases the plasma high density lipoprotein cholesterol (HDL-C) level in mice. However, little is known about the functional quality of HDL particles after EL inhibition. Therefore, the present study assessed the functional quality of HDL isolated from *EL*$^{-/-}$ and wild-type (WT) mice. Anti-inflammatory functions of HDL from *EL*$^{-/-}$ and WT mice were evaluated by in vitro assays. The HDL functions such as PON-1 or PAF-AH activities, inhibition of cytokine-induced vascular cell adhesion molecule-1 expression, inhibition of LDL oxidation, and the ability of cholesterol efflux were similar in HDL isolated from WT and *EL*$^{-/-}$ mice. In contrast, the lipopolysaccharide-neutralizing capacity of HDL was significantly higher in *EL*$^{-/-}$ mice than that in WT mice. To evaluate the anti-inflammatory actions of HDL in vivo, lipopolysaccharide-induced systemic inflammation was generated in these mice. *EL*$^{-/-}$ mice showed higher survival rate and lower expression of inflammatory markers than WT mice. Intravenous administration of HDL isolated from *EL*$^{-/-}$ mice significantly improved the mortality after lipopolysaccharide injection in WT mice. In conclusion, targeted disruption of EL increased HDL particles with preserved anti-inflammatory and anti-atherosclerotic functions. Thus, EL inhibition would be a useful strategy to raise 'good' cholesterol in the plasma.**—Hara, T., T. Ishida, Y. Kojima, H. Tanaka, T. Yasuda, M. Shinohara, R. Toh, and K-i. Hirata. **Targeted deletion of endothelial lipase increases HDL particles with anti-inflammatory properties both in vitro and in vivo. *J. Lipid Res.* 2011.** 52: **57–67.**

Supplementary key words high density lipoprotein • inflammation • lipopolysaccharide • endotoxin shock • adhesion molecule

High plasma levels of high density lipoprotein cholesterol (HDL-C) are known to protect against the development of atherosclerosis and are widely documented as a 'negative risk factor' for coronary heart diseases (1). The anti-atherogenic action of HDL is principally attributable to the reverse transport of cholesterol, whereby HDL promotes the efflux of cholesterol from peripheral cells to the liver. In addition, the HDL particle itself has a variety of anti-inflammatory and anti-oxidative properties. For example, HDL improves endothelial function by stimulating endothelial nitric oxide production. In addition, it inhibits the expression of cell adhesion proteins such as vascular cell adhesion molecule-1 (VCAM-1), intercellular adhesion molecule-1, and E-selectin, and thereby can inhibit inflammatory infiltrates accumulating in the vessel wall (2). Moreover, HDL can directly neutralize lipopolysaccharides (LPSs) derived from Gram-negative bacteria and inhibit the subsequent production of inflammatory cytokines (3).

A number of therapeutic strategies are being developed to target HDL-C in an attempt to inhibit the progression or induce regression of atherosclerosis and reduce cardiovascular events. However, it has been postulated that HDL particles undergo oxidation, chloralization, nitration, and calbamilation under conditions with inflammation, diabetes, and cardiovascular diseases. The HDL particle with these modifications may lose its atheroprotective effects

This research was supported by a Grant for Initiatives for Attractive Education in Graduate Schools: "Program of Raising Young Research Leaders in Biomedical Sciences," a Grants-In-Aid for Scientific Research, a Grant for 21st Century COE Program from the Ministry of Education, Culture, Sports, Science and Technology of Japan, and the Japan Foundation of Cardiovascular Research.

Manuscript received 12 May 2010 and in revised form 23 September 2010.

Published, JLR Papers in Press, October 5, 2010
DOI 10.1194/jlr.M008417

Abbreviations: AA, arachidonic acid; apo, apolipoprotein; EL, endothelial lipase; EPA, eicosapentaenoic acid; HDL-C, high density lipoprotein cholesterol; HDL-*EL*$^{-/-}$, HDL isolated from *EL*$^{-/-}$ mice; HDL-WT, HDL isolated from wild-type mice; HUVEC, human umbilical vein endothelial cell; IL, interleukin; iNOS, inducible nitric oxide synthase; LAL, Limulus amebocyte lysate; LPS, lipopolysaccharide; MPO, myeloperoxidase; PAF-AH, platelet-activating factor acetylhydrolase; plasma-WT, plasma obtained from wild-type mice; plasma-*EL*$^{-/-}$, plasma obtained from *EL*$^{-/-}$ mice; PON, paraoxonase; SFA, saturated fatty acid; TMB, tetramethylbenzine; TNF, tumor necrosis factor; T_{max}, maximum time; VCAM, vascular cell adhesion molecule; W/D, wet-to-dry weight, WT, wild-type.

[1]To whom correspondence should be addressed.
e-mail: ishida@med.kobe-u.ac.jp

and promote inflammatory processes and is referred to as dysfunctional HDL (2). These lines of evidence have stimulated tremendous interest in the functional quality and therapeutic potential of HDL.

Endothelial lipase (EL) is a new member of the lipase gene family (4, 5). EL exhibits preferential substrate specificity for phospholipids on HDL particles and promotes HDL catabolism (6). In fact, EL-deficient mice ($EL^{-/-}$) showed an elevated plasma HDL-C level, whereas EL overexpression results in a reduced HDL-C level (7, 8). These findings suggest that a selective inhibitor of EL, if available, would be useful to increase plasma HDL-C levels, although little is known concerning the functional qualities of HDL particles after EL inhibition. Therefore, the present study focused on the HDL quality after EL disruption both in in vitro and in vivo inflammatory processes.

MATERIALS AND METHODS

Cell culture

Human umbilical vein endothelial cells (HUVECs), THP-1, and J774 cells were purchased from the American Type Culture Collection (Manassas, VA). For the stimulation assay, subconfluent HUVEC was treated with fresh complete medium containing 10 ng/ml tumor necrosis factor (TNF)-α (Biosource, Camarillo, CA) for 24 h in the presence of mouse plasma (50 μL) or HDL (250 μg of protein).

Murine model of LPS-induced endotoxin shock

All animal studies were performed in accordance with the Institutional Guidelines of Kobe University and the Institute for Laboratory Animal Research (ILAR) Guide for the Care and Use of Laboratory Animals. Eight- to twelve-week-old male $EL^{-/-}$ mice (7), which were bred with the C57Bl/6 background more than 25 times, and age-matched male wild-type (WT) C57BL/6 mice (Japan Charles River, Osaka, Japan) were used in this study. The body weight of $EL^{-/-}$ and WT mice at 8 weeks of age was 24.5 ± 2.4 and 27.9 ± 0.9 g (NS, not significant), respectively, and that at 12 weeks of age was 31.0 ± 1.6 and 33.2 ± 3.0 g (NS), respectively. Plasma was obtained from WT mice (Plasma-WT) and $EL^{-/-}$ mice (Plasma-$EL^{-/-}$) by cardiac puncture, and HDL fraction was obtained from the pooled plasma of WT mice (HDL-WT) and $EL^{-/-}$ mice (HDL-$EL^{-/-}$) by ultracentrifugation as described elsewhere (9).

A mouse model of LPS-induced endotoxin shock was generated as described previously (10, 11) Briefly, WT and $EL^{-/-}$ mice were injected intraperitoneally with 20–80 mg/kg of LPS from *Escherichia coli*, serotype 055:B5 (Sigma-Aldrich, St. Louis, MO). Control animals were injected with normal saline (vehicle). Survival of the mice was assessed every 12 h up to 10 days. In a subset of in vivo HDL administration experiments, HDL-WT or HDL-$EL^{-/-}$ was injected through the tail vein (7.5 mg protein/kg), followed by injection of LPS (80 mg/kg, ip).

Cholesterol efflux study

J774 cells were incubated in DMEM containing 0.5% FBS with an Liver X receptor agonist (T0, 3 μmol/L; Sigma-Aldrich) and acetylated low density lipoprotein (50 μg protein/ml) for 24 h. Then, cholesterol efflux was performed for 8 h at 37°C in DMEM/0.2% BSA with the 250 μg/ml of HDL-WT or HDL-$EL^{-/-}$. At the end of the 8 h incubation, the lipid fractions were extracted from the efflux medium or cells by the Bligh and Dyer method (12) followed by the calculation of cholesterol efflux as previously reported (13).

Plasma cytokine and corticosterone determination

$EL^{-/-}$ and WT mice were given an intraperitoneal injection of LPS (40 mg/kg) or vehicle. Two hours later, the plasma was isolated and immediately frozen at −80°C. Plasma levels of cytokine and corticosterone levels were determined by using Q-plex® mouse cytokine array (Biolegend, Santa Fe, CA) and a Coat-A-Count corticosterone kit (Diagnostic Products, Los Angeles, CA), respectively.

Peritoneal macrophages were collected from WT and $EL^{-/-}$ mice 4 days after an intraperitoneal injection of 1 ml of 4% thioglycollate medium. The mouse peritoneal macrophages or human THP-1 cells were stimulated with LPS, and mouse or human TNF-α production in the culture medium was measured using a commercially available kit from R&D Systems (Minneapolis, MN) or Biosource (Camarillo, CA), respectively.

Immunoblot and histological analyses

Western blotting was performed using anti-VCAM-1 (Santa Cruz Laboratory, Santa Cruz, CA), inducible nitric oxide synthase (iNOS) (BD Transduction Laboratories, Bedford, MA), apolipoprotein (apo)A-1 (Abcam, Cambridge, UK), or anti-β-actin antibody (Sigma-Aldrich) as described previously (14). The relative densities of the acquired bands were determined by using the ImageJ software version 1.38 from the National Institutes of Health (available on the World Wide Web).

For histology, mice were euthanized with an overdose of pentobarbital, and the lungs were removed followed by the inflation at a pressure of 20 cm water with 4% paraformaldehyde/PBS. Lungs were fixed overnight, embedded in paraffin, sectioned, and stained with hematoxylin and eosin.

Real-time PCR

Quantitative real-time PCR was performed as previously reported (14). PCR primers for mouse *TNF-α* and *GAPDH* were purchased from Takara-Bio Perfect Real Time Support System (Takara, Shiga, Japan).

Lung wet-to-dry weight ratio and myeloperoxidase activity

A lung wet-to-dry weight (W/D) ratio was used as a parameter of lung water accumulation after the LPS injection as previously described (11). Briefly, lung wet weight was determined immediately after removal of the lung. Lung dry weight was determined after the lung had been completely dried in an oven at 50°C for 24 h. Lung myeloperoxidase (MPO) activity was analyzed as previously reported (11).

Hemodynamic and echocardiographic studies

Six hours after the LPS (20 mg/kg) injection, heart rate and systolic blood pressure were measured by the tail-cuff method. Transthoracic 2-dimensional echocardiography (SONOS 5500, Philips, Andover, MA) was performed under light anesthesia with Avertin (0.005 ml/g of 2.5% solution, ip) 8 h following the LPS (20 mg/kg) challenge (15).

LPS neutralizing capacity

Mouse plasma (5 μl) or HDL (10 μg) were preincubated with 100 ng/ml of LPS at 37°C for 1 h, and then Limulus amebocyte lysate (LAL) activity of LPS was analyzed using an LAL assay kit (QCL-1000, Lonza, Williamsport, PA).

Assays for evaluating the HDL binding to LPS

An in vitro assay was used to quantify the LPS-binding capacity of HDL as previously reported (16). In brief, isolated HDL was

immobilized for 2 h at 37°C on 96-well plates. Nonspecific binding was blocked with 1% BSA for 1 h at 37°C. LPS was biotinylated with EZ-link™ Biotin-LC-Hydrazide (Pierce, Rockford, IL) and incubated for 1 h at 37°C. After washing the plates, the bound LPS was detected by addition of streptavidin-peroxidase and tetramethylbenzidine (TMB).

Analysis of PON-1 and PAF-AH enzymatic activities

Paraoxonase (PON) and arylesterase activities of PON-1 were analyzed spectrophotometrically as previously reported (17). Platelet-activating factor acetylhydrolase (PAF-AH) activity was measured using by commercially available kit (Cayman Chemicals, Ann Arbor, MI).

Cu^{2+}-induced LDL oxidation

Human LDL (density, 1.019–1.063 g:ml) was isolated from the plasma of healthy volunteers by sequential ultracentrifugation as described previously (18). LDL (100 μg/ml) in PBS was incubated with freshly prepared CuSO4 (5 μmol/L) at 37°C in the presence or absence of the isolated HDL (50 μg/ml). Diene formation was measured as the increase in absorbance at 234 nm every 5 min, monitored by a spectrophotometer (UV-1600, Shimadzu). The lag time and maximum time (T_{max}) were determined as described previously (18).

Analysis of HDL particles and fatty acid composition

Concentrations of phospholipids, cholesterol, and triglycerides in the isolated HDL fraction were measured using by the commercially available kits (Wako, Osaka, Japan). The apolipoprotein in the HDL fraction was analyzed by SDS-PAGE (7). Fatty acid composition of isolated HDL was performed using gas chromatography as reported elsewhere (19). The HDL particle size was analyzed by HPLC (LipoSEARCH®) from Skylight Biotech, Inc. (Akita, Japan).

Statistics

The results are expressed as the mean ± SEM. The significance of the differences among the experimental groups was determined by a one-way ANOVA followed by the Bonferroni test for multiple comparisons. The level of statistical significance was set at $p < 0.05$.

RESULTS

HDL isolated from *EL*$^{-/-}$ mice shows athero-protective properties in vitro

First, we compared plasma lipid profile between WT and *EL*$^{-/-}$ mice. As shown in **Table 1**, we confirmed that *EL*$^{-/-}$ mice are 59% higher in HDL-C levels than WT mice. HDL-phospholipids were 78% higher in *EL*$^{-/-}$ mice than in WT mice. In addition, HDL particles in *EL*$^{-/-}$ mice were significantly larger than those in WT mice. Thus, HDL-*EL*$^{-/-}$ was found to be rich in cholesterol and phospholipids with increased particle sizes, which is consistent with previous studies (7, 8). Because HDL has been shown to inhibit expression of VCAM-1 induced by pro-inflammatory cytokines (20), we checked the effect of HDL-WT or HDL-*EL*$^{-/-}$ on the cytokine-induced VCAM-1 expression in HUVEC. The VCAM-1 expression induced by TNF-α was markedly reversed by coincubation with HDL-WT and HDL-*EL*$^{-/-}$ (**Fig. 1A**). There was no difference in the inhibitory effect between HDL-WT and HDL-*EL*$^{-/-}$.

TABLE 1. Plasma lipid profile and HDL characteristics in WT and *EL*$^{-/-}$ mice

	WT	*EL*$^{-/-}$
Total cholesterol	81.4 ± 4.2	129.3 ± 5.8[b]
HDL-cholesterol (mg/dl)	69.8 ± 2.2	111.2 ± 3.2[b]
LDL- cholesterol (mg/dl)	7.3 ± 0.8	11.1 ± 2.1[a]
VLDL- cholesterol (mg/dl)	4.1 ± 0.7	6.0 ± 1.6
Total triglycerides	36.6 ± 4.0	43.6 ± 4.1
HDL-triglycerides (mg/dl)	3.9 ± 0.2	4.5 ± 0.2
LDL- triglycerides (mg/dl)	4.6 ± 0.5	5.7 ± 1.0
VLDL- triglycerides (mg/dl)	28.1 ± 3.8	33.4 ± 4.9
Total phospholipids	166.5 ± 4.8	297.9 ± 8.4[b]
HDL-phospholipids (mg/dl)	151.2 ± 3.4	269.8 ± 4.5[b]
LDL- phospholipids (mg/dl)	8.1 ± 2.2	14.9 ± 2.6[a]
VLDL- phospholipids (mg/dl)	7.2 ± 1.6	13.2 ± 3.9[a]
HDL particle size (nm)	10.97 ± 0.21	11.52 ± 0.30[a]

The HDL fraction was obtained by ultracentrifugation using pooled plasma, and levels of cholesterol, triglyceride, and phospholipid were determined by standard biochemical assays. The HDL particle size was measured by HPLC.

[a] $p < 0.05$.

[b] $p < 0.01$ versus WT mice (n = 8).

Next, we assessed the effect of HDL on Cu^{2+}-induced oxidation of LDL and found no difference in the anti-oxidative effects between HDL-*EL*$^{-/-}$ and HDL-WT (Fig. 1B); the lag time in HDL-*EL*$^{-/-}$ and HDL-WT was 44.8 ± 5.6 versus 46.7 ± 4.5 s; the *T*max was 107.1 ± 6.9 versus 115.7 ± 2.2 s, respectively. Furthermore, we checked the plasma activities of HDL-associated anti-oxidative enzymes including PON-1 and PAF-AH. Both paraoxonase and arylesterase activities were significantly higher in the Plasma-*EL*$^{-/-}$ than those in Plasma-WT (top panels in Fig. 1C, D), which appeared to be in proportion to the HDL-C levels in these mice. However, those activities in HDL were similar if the same amounts of HDL protein were evaluated (bottom panels in Fig. 1C, D), which may reflect the comparative anti-oxidative properties of HDL particles against Cu^{2+}-induced LDL oxidation (21). Similarly, the PAF-AH activities were significantly higher in Plasma-*EL*$^{-/-}$ than those in Plasma-WT, whereas those activities in HDL were similar if the same protein amounts of HDL-*EL*$^{-/-}$ or HDL-WT were evaluated (Fig. 1E). In addition, we assessed the ability of HDL-WT and HDL-*EL*$^{-/-}$ in cholesterol efflux but observed no difference (19.1 ± 4.6, 24.1 ± 4.3%, *P* = NS).

LPS-neutralizing capacity of plasma and HDL are increased in *EL*$^{-/-}$ mice

It is well known that HDL can form a complex with LPS (22), which results in neutralization of its activity and attenuation of the subsequent release of inflammatory cytokines including TNF-α, interleukin (IL)-1, and IL-6 (23). Therefore, we compared the LPS-neutralizing capacity utilizing LAL assays (24). This assay revealed that the plasma LPS-neutralizing capacity was higher in *EL*$^{-/-}$ mice than that in WT mice (**Fig. 2A**, top panel). To determine the relative effects of the plasma HDL-C level on the LPS-neutralizing capacity compared with the alteration in HDL quality, we evaluated the LPS-neutralizing capacity in a same amount of protein, cholesterol, or phospholipids, of HDL-WT and HDL-*EL*$^{-/-}$. Interestingly, HDL-*EL*$^{-/-}$ showed an increase in the LPS-neutralizing capacity when compared with

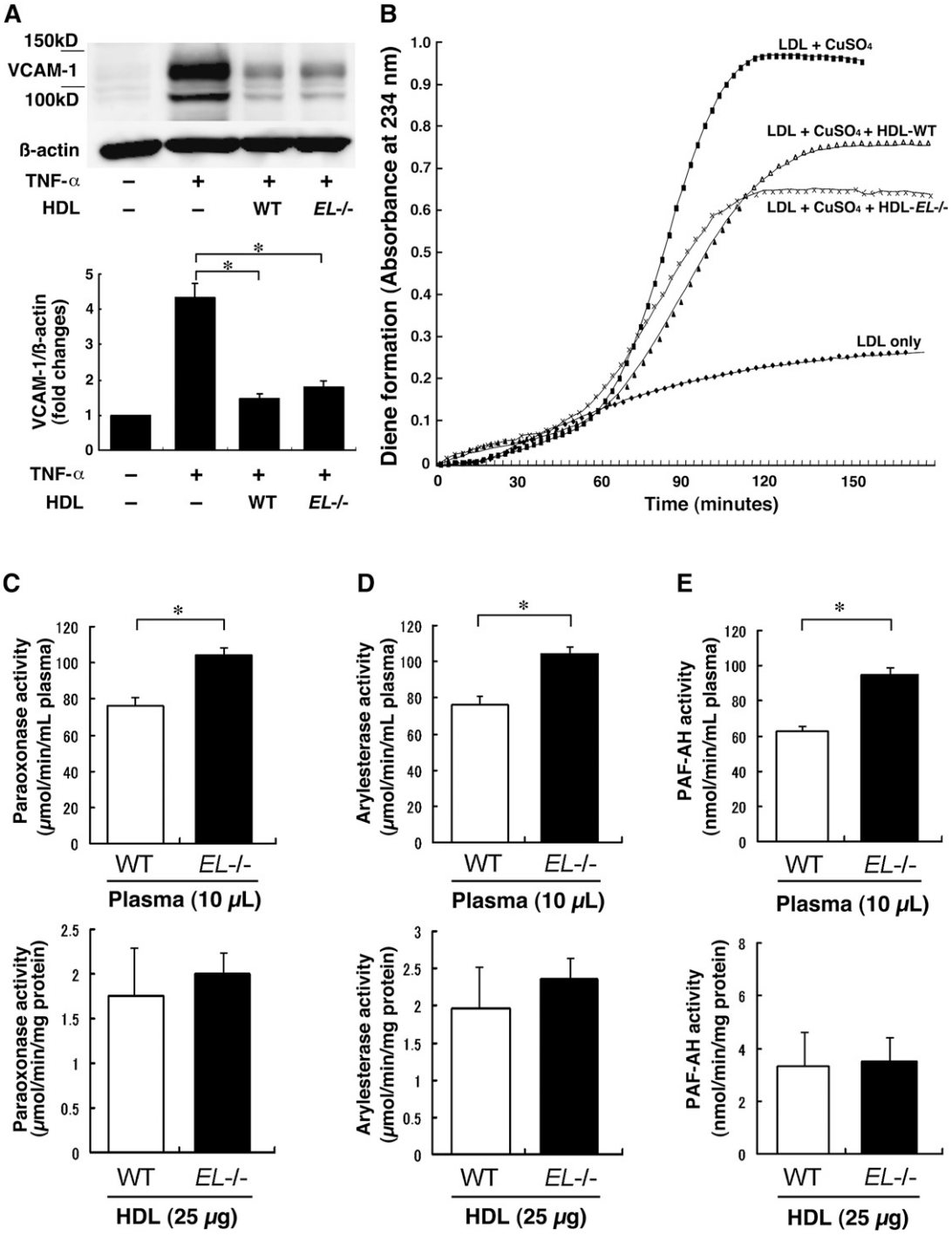

Fig. 1. Anti-inflammatory properties of HDL in control and $EL^{-/-}$ mice. A: Human umbilical vein endothelial cells (HUVECs) were stimulated with tumor necrosis factor (TNF)-α (10 ng/ml) or vehicle for 24 h with HDL (250 μg of protein) isolated from wild-type (WT) (HDL-WT) or $EL^{-/-}$ mice (HDL-$EL^{-/-}$). Both HDL-WT and HDL-$EL^{-/-}$ inhibited the cytokine-induced vascular cell adhesion molecule (VCAM)-1 expression. B: Inhibition of Cu^{2+}-induced LDL oxidation by HDL. LDL (100 μg/ml) was incubated with 2.5 μmol/L copper at 37°C in the absence or presence of the isolated HDL (50 μg protein/ml). Both HDL-WT and HDL-$EL^{-/-}$ inhibited the LDL oxidation. C–E: Activities of HDL-associated enzymes, PON-1 (paraoxanase, C; arylesterase, D) and platelet-activating factor acetylhydrolase (PAF-AH) (E), were determined in the plasma or HDL of WT or $EL^{-/-}$ mice. Bars represent mean ± SEM. * $p < 0.05$ (n = 10 for whole plasma, and n = at least 3 for HDL from pooled plasma).

HDL-WT with the equivalent protein (Fig. 2A, second panel). Notably, apoA-1 content in HDL fraction was similar between HDL-$EL^{-/-}$ and HDL-WT (Fig. 2B) when the equivalent protein was evaluated by SDS-PAGE. The finding indicates that the increased LPS-neutralizing capacity of Plasma-$EL^{-/-}$ does not merely reflect the increase in the plasma HDL-C or apoA-1 levels in $EL^{-/-}$ mice. There was no difference in the LPS-neutralizing capacity between HDL-$EL^{-/-}$ and HDL-WT (Fig. 2A, third and fourth panels) when the equivalent cholesterol or phospholipids were evaluated.

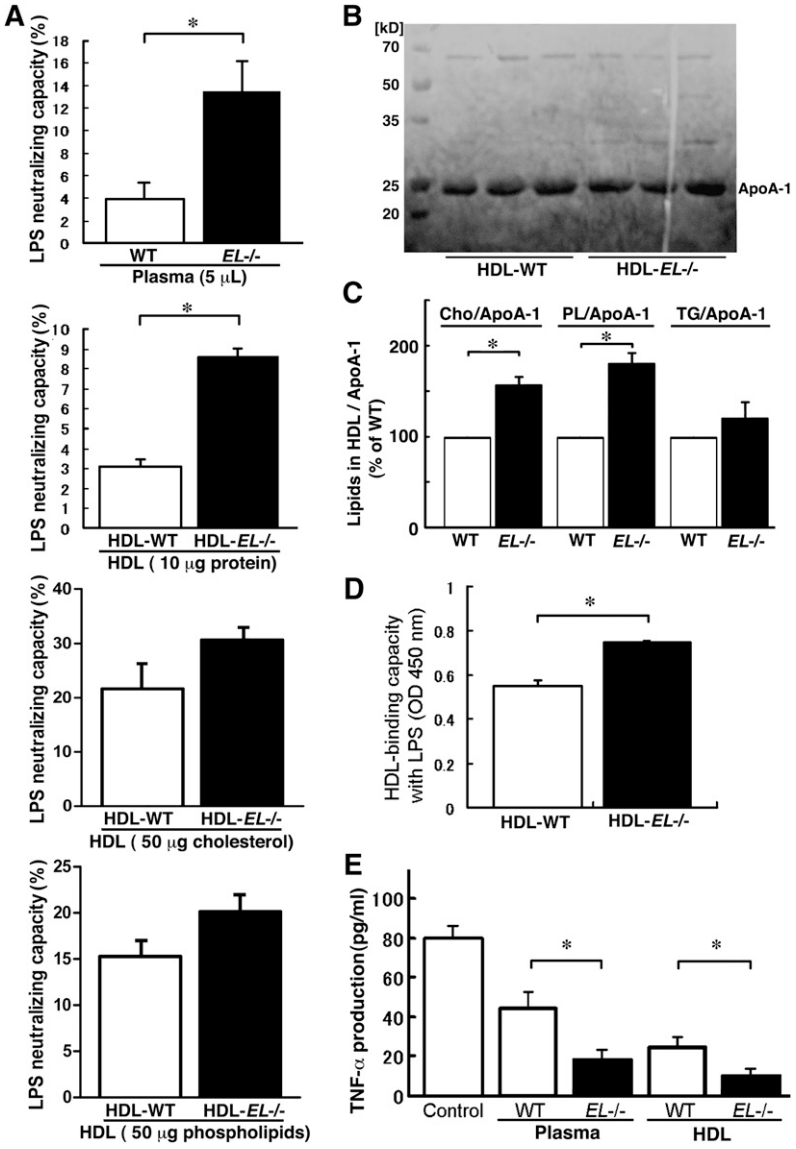

Fig. 2. LPS-neutralizing capacity of HDL was higher in $EL^{-/-}$ mice. A: Mouse plasma (5 μl) or HDL (10 μg protein, 50 μg cholesterol, or 50 μg phospholipids) were incubated with 100 ng/ml of LPS at 37°C for 1 h, and lipopolysaccharide (LPS) neutralization was quantified by the Limulus amebocyte lysate (LAL) assay. B: Apolipoprotein (apo)A-1 protein levels in HDL fractions were similar between HDL-WT and HDL-$EL^{-/-}$ when the same concentration of HDL protein (15 μg protein) was evaluated by SDS-PAGE. C: Concentration of cholesterol (Cho), phospholipids (PL), and triglycerides (TG), as well as apoA-1 content in isolated HDL were determined, and the ratio of Cho/apoA-1, PL/apoA-1, or TG/apoA-1 were expressed as a percent value of WT group. D: Isolated HDL was immobilized to 96-well plates and incubated with biotinylated LPS. Bound LPS was detected by peroxidase-conjugated streptavidin and tetramethylbenzidine (TMB). Binding of LPS to HDL is expressed as a value with OD450 nm. E: THP-1 cells were preincubated with plasma (20 μl) or HDL (50 μg) of WT or $EL^{-/-}$ mice and then treated with 1 μg/ml of LPS. The TNF-α concentration in culture medium was analyzed by ELISA. Bars represent mean ± SEM. * $p < 0.05$ (n = 5–6).

Previous studies have demonstrated that the phospholipid bilayer of the HDL surface can bind to the lipid-A, an anchor protein of LPS, to neutralize its activity (3). To clarify the mechanisms by which HDL-$EL^{-/-}$ has increased LPS-neutralizing capacity, therefore, we compared the lipid content in isolated HDL. HDL-$EL^{-/-}$ was rich in phospholipids and cholesterol (Table 1), whereas the apoA-1 content in HDL fraction was similar in HDL-$EL^{-/-}$ and HDL-WT (Fig. 2B). As a result, we found that the phospholipid- or cholesterol-content in the HDL particle, which was calibrated with apoA-1 content, was markedly higher in HDL-$EL^{-/-}$ than that in HDL-WT (Fig. 2C). Moreover, we directly assessed the interaction of HDL-$EL^{-/-}$ or HDL-WT with LPS. LPS binding capacity of HDL was significantly higher in HDL-$EL^{-/-}$ than in HDL-WT (Fig. 2D). These findings support the notion that the LPS-binding and neutralization are associated with the increase in the phospholipid- or cholesterol-content in the HDL particle. Furthermore, we checked the subsequent cytokine production by comparing LPS-induced TNF-α production in THP-1 cells. Preincubation of the LPS with Plasma-$EL^{-/-}$ or HDL-$EL^{-/-}$ resulted in a significant decrease in the TNF-α production when compared with that observed with Plasma-WT or HDL-WT, respectively (Fig. 2E). Thus, HDL-$EL^{-/-}$ with high phospholipid content showed high binding affinity with LPS and attenuated the bioactivity of LPS.

Analysis of fatty acid composition of isolated HDL fraction

To extend the understanding of the characteristics of HDL-WT and HDL-$EL^{-/-}$, we assessed fatty acid composition using GC-MS. This high-throughput analysis revealed that *EL* deficiency substantially alters the composition of fatty acids in HDL particles (**Fig. 3A**). Total fatty acid content was significantly higher in HDL-$EL^{-/-}$ than HDL-WT (Fig. 3B), which was likely to reflect the increased phospholipids content in HDL-$EL^{-/-}$.

Fatty acids are shown to modulate inflammatory processes; saturated fatty acids (SFAs) directly stimulate TLR2- or TLR4-receptor signaling (25), and n-3 PUFAs exert a range of anti-inflammatory actions whereas n-6 PUFAs are a source of prothrombotic and pro-inflammatory eicosanoids.

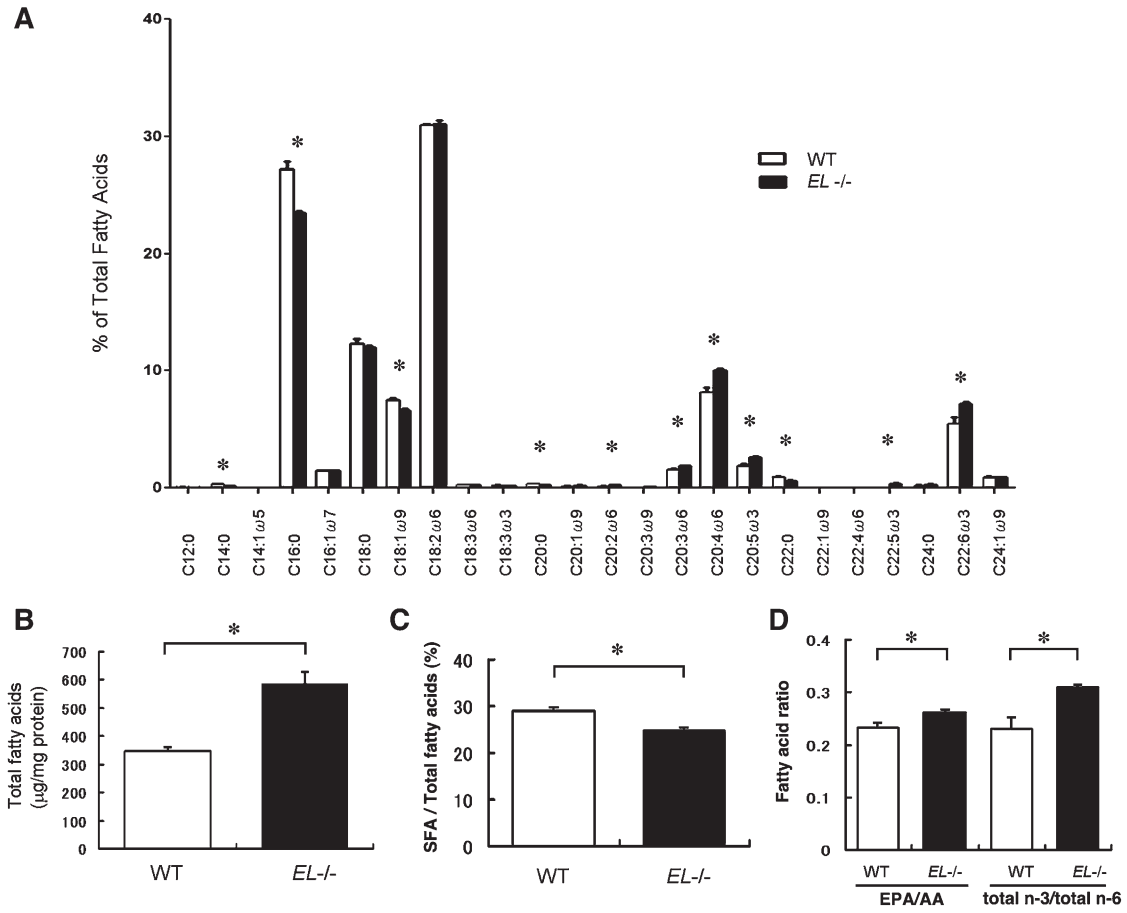

Fig. 3. Analysis of fatty acids composition of isolated HDL. A: Fatty acid composition of isolated HDL was determined by GC-MS. B: Total fatty acids concentration in isolated HDL fractions was higher in HDL-$EL^{-/-}$ than in HDL-WT. C: Ratio of saturated fatty acids (SFA) and total fatty acids was lower in HDL-$EL^{-/-}$ than in HDL-WT. D: eicosapentaenoic acid (EPA)/ arachidonic acid (AA) and n-3/n-6 ratios were higher in HDL-$EL^{-/-}$ than in HDL-WT. Data were shown as mean ± SEM. * $p < 0.05$ versus WT (n = 6).

Interestingly, HDL-$EL^{-/-}$ was significantly lower in SFA than HDL-WT (Fig. 3C). Moreover, both the eicosapentaenoic acid (EPA)/arachidonic acid (AA) ratio and the n-3/n-6 fatty acids ratio were significantly higher in HDL-$EL^{-/-}$ than in HDL-WT (Fig. 3D). These results imply that anti-inflammatory properties of HDL-$EL^{-/-}$ may be partly due to the increased content of the anti-inflammatory fatty acids.

$EL^{-/-}$ mice are protected against endotoxin shock

To evaluate the role of these anti-inflammatory actions of HDL in vivo, LPS-induced systemic inflammation was generated in WT and $EL^{-/-}$ mice. As depicted in **Fig. 4A**, we observed a marked improvement of survival rate in $EL^{-/-}$ mice in response to the relatively high dose (80 mg/kg) of LPS when compared with WT mice. To evaluate the early inflammatory response in these mice, plasma levels of inflammatory cytokines were analyzed 2 h after the LPS injection (40 mg/kg). The LPS injection resulted in robust increases in levels of TNF-α, IL-1β, monocyte chemoattractant protein-1, and IFN-γ both in WT and $EL^{-/-}$ mice (Fig. 4B). However, these cytokine levels were significantly lower in $EL^{-/-}$ mice than in WT mice (Fig. 4B). To determine whether the lower levels of inflammatory cytokines in $EL^{-/-}$ mice reflect the decreased cellular production in response to LPS, we evaluated the LPS-induced TNF-α production in peritoneal macrophages isolated from $EL^{-/-}$ and WT mice. The TNF-α production by $EL^{-/-}$ macrophages was similar to that by WT macrophages in response to LPS (2847.0 ± 119.6 vs. 2663.5 ± 128.3 pg/ml, p = NS). On the other hand, glucocorticoids exert anti-inflammatory effects by suppressing pro-inflammatory cytokines and stimulating anti-inflammatory cytokines. Therefore, we measured plasma corticosterone levels following the LPS injection (40 mg/kg), but found no significant difference between WT and $EL^{-/-}$ mice (528 ± 47.6 vs. 624 ± 29.7 ng/ml, p = NS).

LPS-induced lung damage was attenuated in $EL^{-/-}$ mice

TNF-α mRNA expression in the mouse lung was analyzed following the LPS injection. The LPS injection (25 mg/kg) substantially increased the expression of lung *TNF-α* mRNA levels both in WT and $EL^{-/-}$ mice. Notably, the LPS-induced *TNF-α* expression in $EL^{-/-}$ mice was lower than that in WT mice (**Fig. 5A**). In addition, protein levels of iNOS and VCAM-1 in the lungs were lower in $EL^{-/-}$ mice than WT mice after the LPS injection (Fig. 5B, C)

Histological examination demonstrated that LPS induced an infiltration of numerous polymorphonuclear leukocytes and macrophages in the interstitial spaces and marked swelling of the alveolar walls. These inflammatory

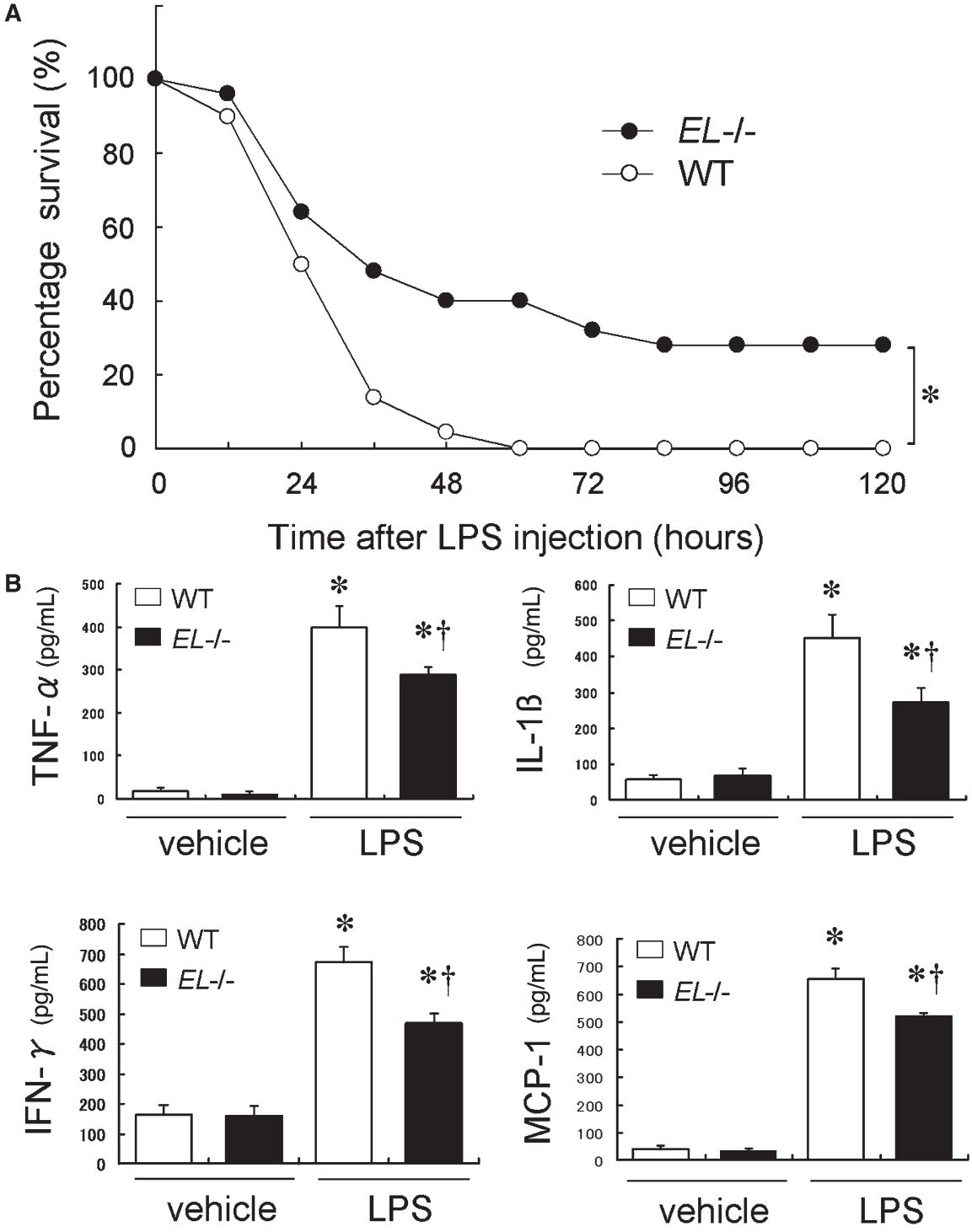

Fig. 4. Effect of *EL* deficiency on LPS-induced mortality and cytokine release. A: Survival rate of WT and $EL^{-/-}$ mice in response to LPS (80 mg/kg). * $p < 0.05$ (n = 25 in each group). B: Plasma cytokine levels 2 h following the LPS or vehicle injection (40 mg/kg). These cytokine productions after LPS challenge were significantly attenuated in $EL^{-/-}$ mice compared with WT. Bars indicate mean ± SEM. * $p < 0.05$ versus baseline, † $p < 0.05$ versus corresponding WT (n = 5 in each group).

changes were attenuated in $EL^{-/-}$ mice (Fig. 5D). We assessed granulocyte infiltration by MPO activity in the lung as well as lung edema by means of the W/D ratio. These parameters were low and similar in the two mouse groups at baseline (Fig. 5E, F). The LPS treatment increased the lung MPO activity, which was significantly lower in $EL^{-/-}$ mice than that in WT mice (Fig. 5E). Moreover, the lung W/D ratio following the LPS injection was lower in $EL^{-/-}$ mice than that in WT mice (Fig. 5F).

EL deficiency attenuates LPS-induced cardiac dysfunction and hypotension

To compare the cardiac inflammation and function, the *TNF-α* mRNA expression in the heart was analyzed following

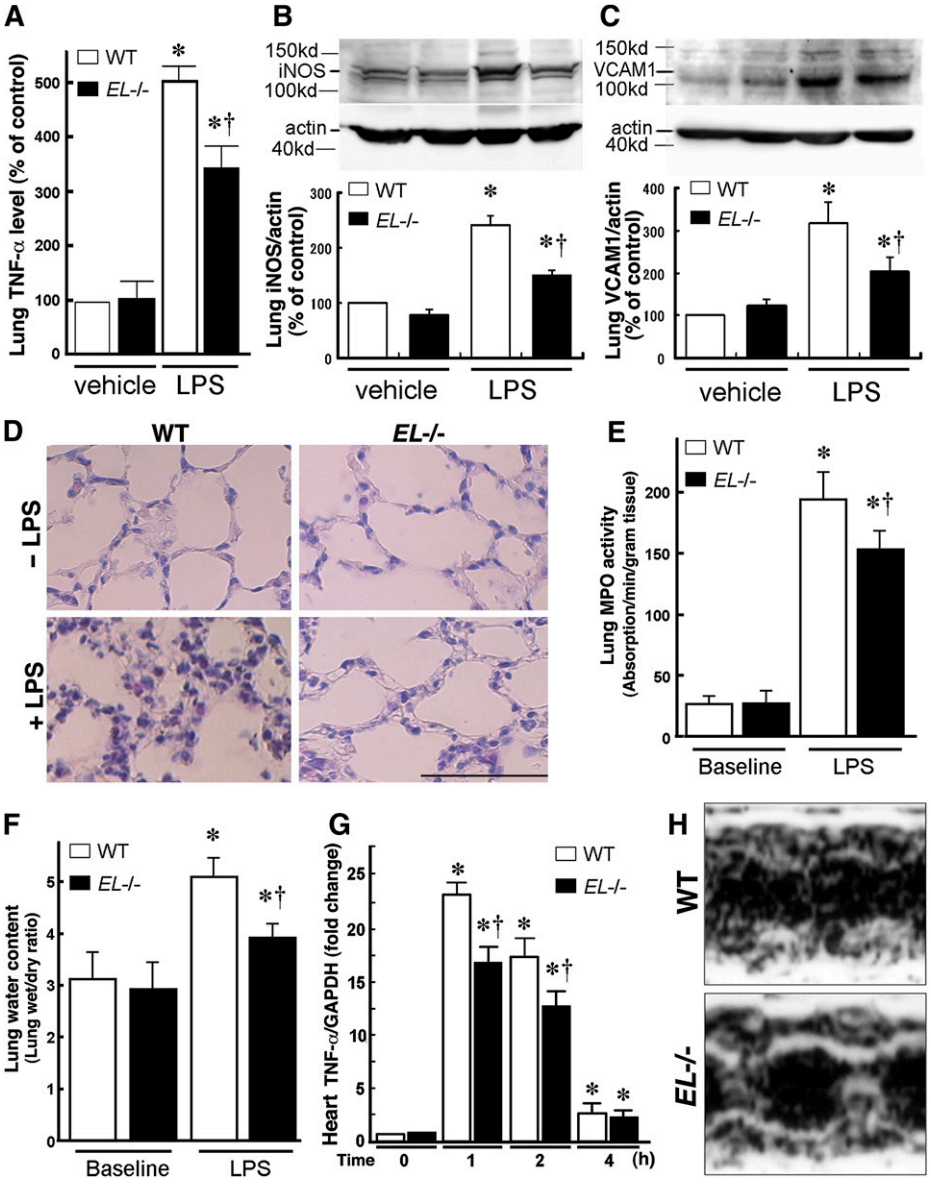

Fig. 5. *EL* deficiency attenuates LPS-induced lung inflammation and heart failure. WT and $EL^{-/-}$ mice were injected with LPS (25 mg/kg). After 24 h, the lungs and heart were excised for expression analyses. A: Real-time PCR revealed that the LPS-induced *TNF*-α mRNA expression in the lung was attenuated in $EL^{-/-}$ mice compared with WT mice. Western blotting revealed that iNOS (B) and VCAM-1 (C) inductions in the lung were attenuated in $EL^{-/-}$ compared with WT mice. Values are expressed as percent of control (WT mice at baseline). D: Lung histology before and 24 h following the LPS injection. Note marked infiltration of polymorphonuclear leukocytes and macrophages in the interstitial spaces and swelling of the alveolar walls, and the LPS-induced damage was attenuated in $EL^{-/-}$ mice. The bar indicates 50 μm. Lung myeloperoxidase (MPO) activity (E) and lung wet/dry ratio (F) were significantly lower in $EL^{-/-}$ mice than in WT mice in response to the LPS administration. G: The LPS-induced *TNF*-α expression in the heart was attenuated in $EL^{-/-}$ mice compared with WT mice (n = 5 in each group). Bars indicate mean ± SEM. * $p < 0.05$ versus baseline, † $p < 0.05$ versus corresponding WT mice (n = 6). H: Representative images of cardiac echocardiography of WT and $EL^{-/-}$ mice after the LPS challenge.

the LPS injection. The LPS injection (25 mg/kg) substantially increased the expression of the heart *TNF-α* mRNA both in WT and $EL^{-/-}$ mice, and the expression returned to the basal level 4 h after the LPS challenge (Fig. 5G). In $EL^{-/-}$ mice, the *TNF-α* induction was attenuated compared with WT mice 1 and 2 h after the LPS administration (Fig. 5G). Moreover, we measured blood pressure and performed echocardiographic examinations in these mice and found no difference in blood pressure between two groups at the baseline. However, blood pressure fell from 106.8 ± 5.5 to 90.6 ± 7.6 mmHg ($p < 0.05$) by the LPS challenge in WT mice. In contrast, the blood pressure was not affected by the LPS treatment in $EL^{-/-}$ mice (from 108.7 ± 2.5 to 108.4 ± 2.5 mmHg, p = NS). The echocardiography revealed that the fractional shortening of the left ventricle after the LPS challenge was significantly lower in WT than in $EL^{-/-}$ mice

(23.0 ± 5.1% vs. 34.8 ± 2.1%, $p < 0.05$, Fig. 5H), indicating that the cardiac contractility was preserved in $EL^{-/-}$ mice.

Administration of HDL-$EL^{-/-}$ improved survival in LPS-induced septic shock

We investigated if the improved survival in $EL^{-/-}$ mice was attributable to the increase in anti-inflammatory HDL particles. WT mice were administered the same amount of HDL-$EL^{-/-}$ or HDL-WT from the tail vein followed by the LPS treatment and the survival rate was monitored. Both HDL-WT and HDL-$EL^{-/-}$ improved the survival rate in the septic shock model compared with vehicle treatment (**Fig. 6**). Interestingly, the survival rate was significantly higher in the case of HDL-$EL^{-/-}$ than in HDL-WT. These findings indicate that the improved anti-inflammatory function of HDL-$EL^{-/-}$ is relevant in the in vivo endotoxin shock model, and that *EL* deletion may increase HDL-C with augmented LPS-neutralizing capacity and preserved anti-inflammatory properties.

DISCUSSION

In the present study, we showed that targeted disruption of EL results in an increase not only in plasma HDL-C levels but also in the HDL quality; HDL-$EL^{-/-}$ had a variety of anti-inflammatory properties, in terms of inhibition of VCAM-1 expression, the HDL-associated anti-oxidative enzymatic activities, and the ability of cholesterol efflux, whereas the anti-inflammatory potency was similar between HDL-WT and HDL-$EL^{-/-}$. Moreover, HDL-$EL^{-/-}$ exhibited a higher LPS-neutralizing capacity than HDL-WT. These anti-inflammatory actions of HDL appear to be physiologically relevant in vivo because $EL^{-/-}$ mice showed an attenuation in inflammatory responses after the LPS challenge, resulting in the increased survival rate against endotoxin shock.

Although many of the anti-inflammatory functions of HDL were similar between $EL^{-/-}$ and WT mice, only LPS-neutralizing capacity was more potent in HDL-$EL^{-/-}$ than in HDL-WT. Previous studies have demonstrated that lipid-A binds to the phospholipids of the HDL surface (3). In fact, the present study has shown that phospholipid content in HDL particles was higher in HDL-$EL^{-/-}$ than in HDL-WT, which is in line with past reports (8, 26). Therefore, we speculate that the increased phospholipid content may increase the affinity of the HDL particles to lipid-A and then neutralize bioactivity of LPS. Furthermore, HDL-$EL^{-/-}$ was rich in n-3 PUFAs including EPA and poor in SFA compared with HDL-WT, which is likely to make the HDL particles more anti-inflammatory. The precise mechanism underlying the altered fatty acid composition remains unclear and needs to be clarified by further studies. However, the change in HDL fatty acids suggests that the selectivity of EL phospholipase activity may depend on the fatty acid composition in the substrate HDL phospholipids. On the other hand, previous studies have indicated that apoA-1 itself can neutralize LPS (27). Because the apoA-1 content relative to the protein content was similar in HDL-WT and HDL-$EL^{-/-}$, it is considered that the anti-inflammatory effect of HDL-$EL^{-/-}$ is not likely mediated by the change in apoA-1 content. It has been reported that suppression of EL in macrophages directly decreases the secretion of inflammatory cytokine secretion (28, 29). In the present study, however, there was no difference in TNF-α production by isolated macrophages between $EL^{-/-}$ and WT mice.

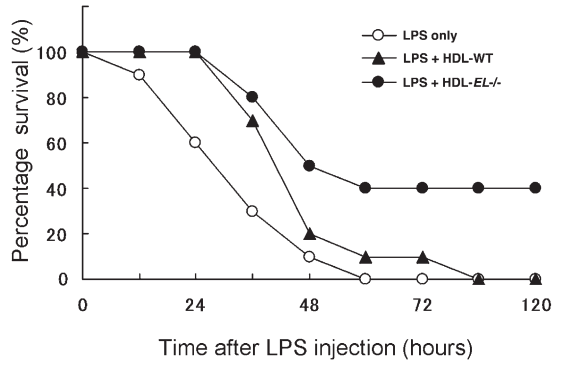

Fig. 6. Administration of HDL-$EL^{-/-}$ improved LPS-induced mortality. HDL isolated from WT (HDL-WT) or $EL^{-/-}$ mice (HDL-$EL^{-/-}$) were injected to WT mice through the tail vein (7.5 mg protein/kg), followed by the LPS administration (80 mg/kg, ip). Mice were carefully monitored, and survival rate at various times was recorded (n = 10 in each group, $p < 0.05$).

In endotoxin-induced systemic inflammation, LPS is known to inhibit activities of LPL and HL to increase plasma levels of apoB-containing lipoproteins such as VLDL and its remnants (30–32). Also, LPS increases EL expression to decrease HDL levels (10). Thus, EL may modulate the severity of endotoxin shock through plasma HDL levels. Kitchens et al. (33) have reported that in spite of the decline in HDL levels, HDL remains the dominant LPS acceptor in septic patients, whereas LPS binding shifts to VLDL in some cases. They also reported that the LPS binding and neutralization are largely associated with phospholipid content in lipoprotein subclasses (33). These findings support that EL disruption may not only increase HDL quantity but also improve HDL quality, and as a result, protect against endotoxin shock.

Constitutive knockout mice are often accompanied by compensatory changes. In fact, Ma et al. (8) have previously demonstrated that expressions of LPL and HL are increased in $EL^{-/-}$ mice, although we found no difference in LPL or HL levels between WT and $EL^{-/-}$ mice (34). In addition, they have demonstrated that hepatic production of LCAT is increased in $EL^{-/-}$ mice without changing plasma LCAT levels (8). Because each of these molecules is a regulator of HDL metabolism, an alteration of the expression, if any, would affect the quality and quantity of HDL in $EL^{-/-}$ mice. Further studies are required to investigate the effects of the compensatory changes on HDL metabolism.

The effect of EL deficiency on atherogenesis has been reported previously. We have reported that EL deficiency protected against atherosclerosis in $apoE^{-/-}$ mice by raising plasma HDL levels and inhibiting monocyte-vascular interactions (10, 35). However, another group has reported that EL deficiency did not affect atherogenesis in $apoE^{-/-}$ or

LDL-receptor$^{-/-}$ mice, despite the increase in plasma HDL levels (36). Thus, the effect of EL on the atherogenesis remained controversial. The present study supports that increased HDL in *EL*$^{-/-}$ mice has anti-atherosclerotic actions as WT-HDL does.

Plasma EL mass was inversely correlated with plasma HDL-C levels in humans (37, 38). Edmondson et al. (39) have recently reported that loss-of-function variants of EL are associated with the high plasma level of HDL-C in humans. These findings indicate that EL is a determinant of plasma HDL-C levels in humans. It has been postulated that EL has a variety of direct functions in atherogenesis through promoting LDL uptake in macrophages (40), monocyte adhesion (10, 41), cholesterol uptake to the vascular wall (35), and cholesterol efflux (42), besides hydrolyzing HDL phospholipids. These findings support that pharmaceutical inhibition of EL, if possible, may have not only an HDL-C-raising effect but also direct anti-atherosclerotic effects on the vascular wall. On the contrary, Qiu et al. (43) demonstrated that EL promoted apoA-1-mediated cholesterol efflux, which indicates that inhibition of EL may act as a pro-atherosclerotic function. Moreover, the metabolism and function of HDL in mice largely differ from those in humans. Therefore, further studies are required to elucidate the role of EL in the reverse cholesterol transport system and atherosclerosis in humans. However, the findings presented in this study imply that EL inhibition by pharmaceutical intervention would increase anti-inflammatory HDL particles.

REFERENCES

1. Gordon, T., W. P. Castelli, M. C. Hjortland, W. B. Kannel, and T. R. Dawber. 1977. High density lipoprotein as a protective factor against coronary heart disease. *Am. J. Med.* **62:** 707–714.
2. Barter, P. J., S. Nicholls, K. A. Rye, G. M. Anatharamaiah, M. Navab, and A. M. Fogelman. 2004. Antiinflammatory properties of HDL. *Circ. Res.* **95:** 764–772.
3. Levine, D. M., T. S. Parker, T. M. Donnelly, A. Walsh, and A. Rubin. 1993. In vivo protection against endotoxin by plasma high density lipoprotein. *Proc. Natl. Acad. Sci. USA.* **90:** 12040–12044.
4. Hirata, K., H. L. Dichek, J. A. Cioffi, S. Y. Choi, N. J. Leeper, L. Quintana, G. S. Kronmal, A. D. Cooper, and T. Quertermous. 1992. Cloning of a unique lipase from endothelial cells extends the lipase gene family. *J. Biol. Chem.* **274:** 14170–14175.
5. Jaye, M., K. J. Lynch, J. Krawiec, D. Marchadier, C. Maugeais, K. Doan, V. South, D. Amin, M. Perrone, and D. J. Rader. 1999. A novel endothelial-derived lipase that modulates HDL metabolism. *Nat. Genet.* **21:** 424–428.
6. McCoy, M. G., G. S. Sun, D. Marchadier, C. Maugeais, J. M. Glick, and D. J. Rader. 2002. Characterization of the lipolytic activity of endothelial lipase. *J. Lipid Res.* **43:** 921–929.
7. Ishida, T., S. Choi, R. K. Kundu, K. Hirata, E. M. Rubin, A. D. Cooper, and T. Quertermous. 2003. Endothelial lipase is a major determinant of HDL level. *J. Clin. Invest.* **111:** 347–355.
8. Ma, K., M. Cilingiroglu, J. D. Otvos, C. M. Ballantyne, A. J. Marian, and L. Chan. 2003. Endothelial lipase is a major genetic determinant for high-density lipoprotein concentration, structure, and metabolism. *Proc. Natl. Acad. Sci. USA.* **100:** 2748–2753.
9. Havel, R. J., H. A. Eder, and J. H. Bragdon. 1955. The distribution and chemical composition of ultracentrifugally separated lipoproteins in human serum. *J. Clin. Invest.* **34:** 1345–1353.
10. Kojma, Y., K. Hirata, T. Ishida, Y. Shimokawa, N. Inoue, S. Kawashima, T. Quertermous, and M. Yokoyama. 2004. Endothelial lipase modulates monocyte adhesion to the vessel wall. A potential role in inflammation. *J. Biol. Chem.* **279:** 54032–54038.
11. Yamashita, T., S. Kawashima, Y. Ohashi, M. Ozaki, T. Ueyama, T. Ishida, N. Inoue, K. Hirata, H. Akita, and M. Yokoyama. 2000. Resistance to endotoxin shock in transgenic mice overexpressing endothelial nitric oxide synthase. *Circulation.* **101:** 931–937.
12. Bligh, E. G., and W. J. Dyer. 1959. A rapid method of total lipid extraction and purification. *Can. J. Biochem. Physiol.* **37:** 911–917.
13. Matsuura, F., N. Wang, W. Chen, X. C. Jiang, and A. R. Tall. 2006. HDL from CETP-deficient subjects shows enhanced ability to promote cholesterol efflux from macrophages in an apoE- and ABCG1-dependent pathway. *J. Clin. Invest.* **116:** 1435–1442.
14. Hara, T., T. Ishida, H. M. Cangara, and K. Hirata. 2009. Endothelial cell-selective adhesion molecule regulates albuminuria in diabetic nephropathy. *Microvasc. Res.* **77:** 348–355.
15. Masano, T., S. Kawashima, R. Toh, S. Satomi-Kobayashi, M. Shinohara, T. Takaya, N. Sasaki, M. Takeda, H. Tawa, T. Yamashita, et al. 2008. Beneficial effects of exogenous tetrahydrobiopterin on left ventricular remodeling after myocardial infarction in rats. *Circ. J.* **72:** 1512–1519.
16. Massamiri, T., P. S. Tobias, and L. K. Curtiss. 1997. Structural determinants for the interaction of lipopolysaccharide binding protein with purified high density lipoproteins: role of apolipoprotein A-I. *J. Lipid Res.* **38:** 516–525.
17. Van Himbergen, T. M., M. Roest, J. de Graaf, E. H. Jansen, H. Hattori, J. J. Kastelein, H. A. Voorbij, A. F. Stalenhoef, and L. J. van Tits. 2005. Indications that paraoxonase-1 contributes to plasma high density lipoprotein levels in familial hypercholesterolemia. *J. Lipid Res.* **46:** 445–451.
18. Rikitake, Y., S. Kawashima, S. Takeshita, T. Yamashita, H. Azumi, M. Yasuhara, H. Nishi, N. Inoue, and M. Yokoyama. 2000. Antioxidative properties of fluvastatin, an HMG-CoA reductase inhibitor, contribute to prevention of atherosclerosis in cholesterol-fed rabbits. *Atherosclerosis.* **152:** 79–87.
19. Su, H. M., M. C. Huang, N. M. Saad, P. W. Nathanielsz, and J. T. Brenna. 2001. Fetal baboons convert 18:3n-3 to 22:6n-3 in vivo. A stable isotope tracer study. *J. Lipid Res.* **42:** 581–586.
20. Cockerill, G. W., K. A. Rye, J. R. Gamble, M. A. Vadas, and P. J. Barter. 1995. High-density lipoproteins inhibit cytokine-induced expression of endothelial cell adhesion molecules. *Arterioscler. Thromb. Vasc. Biol.* **15:** 1987–1994.
21. Aviram, M., M. Rosenblat, C. L. Bisgaier, R. S. Newton, S. L. Primo-Parmo, and B. N. La Du. 1998. Paraoxonase inhibits high-density lipoprotein oxidation and preserves its functions. A possible peroxidative role for paraoxonase. *J. Clin. Invest.* **101:** 1581–1590.
22. Rensen, P. C., M. Oosten, E. Bilt, M. Eck, J. Kuiper, and T. J. Berkel. 1997. Human recombinant apolipoprotein E redirects lipopolysaccharide from Kupffer cells to liver parenchymal cells in rats in vivo. *J. Clin. Invest.* **99:** 2438–2445.
23. Pajkrt, D., J. E. Doran, F. Koster, P. G. Lerch, B. Arnet, T. van der Poll, J. W. ten Cate, and S. J. van Devenster. 1996. Antiinflammatory effects of reconstituted high-density lipoprotein during human endotoxemia. *Exp. Med.* **184:** 1601–1608.
24. Cai, L., A. Li, F. C. de Beer, L. R. Tannock, and D. R. van der Westhuyzen. 2008. SR-BI protects against endotoxemia in mice through its roles in glucocorticoid production and hepatic clearance. *J. Clin. Invest.* **118:** 364–375.
25. Shi, H., M. V. Kokoeva, K. Inouye, I. Tzameli, H. Yin, and J. S. Flier. 2006. TLR4 links innate immunity and fatty acid-induced insulin resistance. *J. Clin. Invest.* **116:** 3015–3025.
26. Maugeais, C., U. J. Tietge, U. C. Broedl, D. Marchadier, W. Cain, M. G. McCoy, S. Lund-Katz, J. M. Glick, and D. J. Rader. 2003. Dose-dependent acceleration of high-density lipoprotein catabolism by endothelial lipase. *Circulation.* **108:** 2121–2126.
27. Grunfeld, C., and K. R. Feingold. 2008. HDL and innate immunity: a tale of two apolipoproteins. *J. Lipid Res.* **49:** 1605–1606.
28. Qiu, G., A. C. Ho, W. Yu, and J. S. Hill. 2007. Suppression of endothelial or lipoprotein lipase in THP-1 macrophages attenuates proinflammatory cytokine secretion. *J. Lipid Res.* **48:** 385–394.
29. Wang, X., W. Jin, and D. J. Rader. 2007. Upregulation of macrophage endothelial lipase by toll-like receptors 4 and 3 modulates macrophage interleukin-10 and -12 production. *Circ. Res.* **100:** 1008–1015.
30. White, J. R., A. Chait, S. J. Klebanoff, S. Deeb, and J. D. Brunzell. 1988. Bacterial lipopolysaccharide reduces macrophage lipoprotein lipase levels: an effect that is independent of tumor necrosis factor. *J. Lipid Res.* **29:** 1379–1385.
31. Feingold, K. R., M. Marshall, R. Gulli, A. H. Moser, and C. Grunfeld. 1994. Effect of endotoxin and cytokines on lipoprotein lipase activity in mice. *Arterioscler. Thromb.* **14:** 1866–1872.

32. Feingold, K. R., R. A. Memon, A. H. Moser, J. K. Shigenaga, and C. Grunfeld. 1999. Endotoxin and interleukin-1 decrease hepatic lipase mRNA levels. *Atherosclerosis.* **142:** 379–387.
33. Kitchens, R. L., P. A. Thompson, R. S. Munford, and G. E. O'Keefe. 2003. Acute inflammation and infection maintain circulating phospholipid levels and enhance lipopolysaccharide binding to plasma lipoproteins. *J. Lipid Res.* **44:** 2339–2348.
34. Tanaka, H., T. Ishida, T. P. Johnston, T. Yasuda, T. Ueyama, Y. Kojima, R. K. Kundu, T. Quertermous, Y. Ishikawa, and K. Hirata. 2009. Role of endothelial lipase in plasma HDL levels in a murine model of hypertriglyceridemia. *J. Atheroscler. Thromb.* **16:** 327–338.
35. Ishida, T., S. Y. Choi, R. K. Kundu, J. Spin, T. Yamashita, K. Hirata, Y. Kojima, M. Yokoyama, A. D. Cooper, and T. Quertermous. 2004. Endothelial lipase modulates susceptibility to atherosclerosis in apolipoprotein-E-deficient mice. *J. Biol. Chem.* **279:** 45085–45092.
36. Ko, K. W., A. Paul, K. Ma, L. Li, and L. Chan. 2005. Endothelial lipase modulates HDL but has no effect on atherosclerosis development in apoE−/− and LDLR−/− mice. *J. Lipid Res.* **46:** 2586–2594.
37. Badellino, K. O., M. L. Wolfe, M. P. Reilly, and D. J. Rader. 2006. Endothelial lipase concentrations are increased in metabolic syndrome and associated with coronary atherosclerosis. *PLoS Med.* **3:** e22.
38. Kojima, Y., T. Ishida, L. Sun, T. Yasuda, R. Toh, Y. Rikitake, A. Fukuda, N. Kume, H. Koshiyama, A. Taniguchi, et al. 2010. Pitavastatin decreases the expression of endothelial lipase both in vitro and in vivo. *Cardiovasc. Res.* **87:** 385–393.
39. Edmondson, A. C., R. J. Brown, S. Kathiresan, L. A. Cupples, S. Demissie, A. K. Manning, M. K. Jensen, E. B. Rimm, J. Wang, A. Rodrigues, et al. 2009. Loss-of-function variants in endothelial lipase are a cause of elevated HDL cholesterol in humans. *J. Clin. Invest.* **119:** 1042–1050.
40. Yasuda, T., K. Hirata, T. Ishida, Y. Kojima, H. Tanaka, T. Okada, T. Quertermous, and M. Yokoyama. 2007. Endothelial lipase is increased by inflammation and promotes LDL uptake in macrophages. *J. Atheroscler. Thromb.* **14:** 192–201.
41. Fuki, I. V., N. Blanchard, W. Jin, D. H. Marchadier, J. S. Millar, J. M. Glick, and D. J. Rader. 2003. Endogenously produced endothelial lipase enhances binding and cellular processing of plasma lipoproteins via heparan sulfate proteoglycan-mediated pathway. *J. Biol. Chem.* **278:** 34331–34338.
42. Gauster, M., O. V. Oskolokva, J. Innerlohinger, O. Glatter, G. Knipping, and S. Frank. 2004. Endothelial lipase-modified high-density lipoprotein exhibits diminished ability to mediate SR-B1 (scavenger receptor B type 1)-dependent free-cholesterol efflux. *Biochem. J.* **382:** 75–82.
43. Qiu, G., and J. S. Hill. 2009. Endothelial lipase promotes apolipoprotein A1-mediated cholesterol efflux in THP-1 macrophages. *Arterioscler. Thromb. Vasc. Biol.* **29:** 84–91.